Check for updates

Effect of Ocean Warming on Cloud Properties Over India and Adjoining Oceanic Regions

RUCHITA SHAH[1] and ROHIT SRIVASTAVA[1]

Abstract—Changes in precipitation pattern have been associated with global warming and is of more importance particularly for monsoon dependent regions such as India, which receives maximum rainfall from south-west monsoon. Indian land mass is surrounded by ocean from three sides named Arabian Sea (AS), Bay of Bengal (BOB) and rest of the Indian Ocean (IO) which makes its climate more sensitive. To understand the effect of global warming, long term (1960–2017) annually averaged in-situ sea surface temperature (SST) is studied which shows an increasing trend (~ 0.11 °C/decade; $P < 0.05$) with higher variations ($r^2_{AS} = 0.46$; $r^2_{BOB} = 0.43$) over AS and BOB whereas comparatively lower in magnitude (~ 0.14 °C/decade; $P < 0.05$) with less variation ($r^2_{IO} = 0.74$) over IO. Rise in SST could vary evaporation rate, moisture content, cloud temperature and initial conditions required for cloud formation. To understand this heterogeneity in conjunction with seasonal variation, present study correlates cloud microphysical properties such as cloud effective radius (CER) with SST and aerosol optical depth (AOD) at high-resolution ($1° \times 1°$) using linear interpolation method during 2001–2016. Features of north-east monsoon captures with high ($\sim 0.006–0.012$ kg/kg) specific humidity at 850 hPa, positive correlation ($\sim 0.1–0.8$) of SST-CER and negative correlation (~ -0.1 to ~ -0.8) of AOD–CER over BOB which may imply formation of bigger droplets due to presence of more moisture and less AOD. Though these patches show prominent results, it also shows scattered interpolation signifying role of other parameters on CER. Findings would be promising with more parameters, which can be used as an input data in climate models to understand regional climate variability.

Keywords: Global warming, uneven precipitation pattern, cloud microphysical properties, oceanic regions of India.

1. Introduction

Global warming is a natural process in which radiant energy may transmit, absorb or redirected (reflected or scattered). Emitted solar radiation gets absorb by greenhouse gases, which fasten the vibration of atmospheric molecules and thus cause an increase in the temperature. On the other hand, this generated heat emit as longwave radiation and may further escape out into the space (Tarbuck et al. 1997). Balance between emission of longwave radiation by Earth's surface and emission of solar radiation is important to maintain the temperature of the earth. But recent increasing anthropogenic activities have raised a serious concern towards global temperature rise and hence climate change. In this warming climate, there are various effects of global warming such as rise in SST (IPCC 2013), rise in surface temperature (Nageswararao et al. 2020), increase in humidity at high pressure levels (surface-700 hPa) (Chaboureau et al. 1998), certain types of aerosol (Mitra and Sharma 2002; Aswini et al. 2020; Budhavant et al. 2020), varying wind speed (Vidhya et al. 2020; Zheng et al. 2020), more cloud turbulence (Muhsin et al. 2020), increasing rate of evaporation and condensation (Bretherton et al. 2013; Feingold et al. 2010). Such alteration in atmospheric parameters may vary cloud microphysical processes as well as precipitation patterns. Earlier research studies have reported that concentration of aerosol, their size as well as their type have intense impact on earth's radiation budget (IPCC 2001, 2007; Andreae et al. 2005; Mukherjee et al. 2020; Schill et al. 2020).Moreover, optical properties of aerosol-scattering and absorption also play an important role as it causes direct radiative forcing. Also aerosols of hygroscopic nuclei mostly help to form cloud droplet by triggering condensation process through heterogeneous nucleation. *In-situ* and satellite measurement data together reported that aerosols transported by pollution, may indirectly alter size distribution of cloud droplets and hence cloud microphysical properties (Lohmann and Feichter 2005; Chylek et al. 2006; Shika et al. 2020; Eck et al. 2020). Rising

[1] Department of Science, Pandit Deendayal Petroleum University, Raisan, Gandhinagar, Gujarat, India. E-mail: rohit.prl@gmail.com

aerosol concentration due to anthropogenic activities may increase cloud droplet number concentration and decrease size of cloud droplet at fixed liquid water content, which may also affect precipitation efficiency (Twomey 1977; Andreae 1995; Ansari et al. 2020; Harrison et al. 2020). Along with this, their emission sources (i.e. natural and anthropogenic) vary with spatial and temporal distribution, which might be changing cloud microphysical properties in presently driving climate change (Ramanathan et al. 2001; Kaskaoutis et al. 2011; Tiwari et al. 2015). Thus, role of aerosol is important to know about variation in cloud microphysical properties, which in turn may help to understand cloud formation processes as well as rainfall patterns.

Clouds are source of precipitation and depending on atmospheric conditions, it produce different forms of precipitation such as rain, snow, hail and sleet. The equatorial region in the tropics receives precipitation mostly in the form of rain, as this region is highly governed by a large amount of heat which usually keeps it warm (Su et al. 2017). Earlier study has shown that SST governs precipitation pattern in tropical as well as in subtropical regions (Trenberth and Shea 2005). Rise in SST may increase rate of evaporation which in turn vary moisture content in the atmosphere as availability of moisture plays an important role to understand cloud microphysical properties and hence precipitation pattern. Such studies are quite sensitive for a country like India, situated in northern tropical region and surrounded with ocean from three sides-Arabian Sea from west, Bay of Bengal from east and remaining Indian Ocean from south, which makes its climate more diversified. Earlier studies have reported from The Indian Ocean Experiment (INDOEX) field programs, high polluted aerosol with high concentration of cloud condensation nuclei (CCN) ($> 1500/cm^3$) were observed over Arabian Sea and Bay of Bengal, whereas its concentration gets weaken ($< 200/cm^3$) over rest of the Indian Ocean (Gabriel et al. 2002). Thus, Arabian Sea and Bay of Bengal are usually influenced with high concentration of CCN as compared to remaining portions of Indian Ocean, which also have seasonal dependency (Tiwari et al. 2016). Hence, study of activation of aerosol, concentration of CCN, type of CCN as well as meteorological conditions may help

to understand spatial–temporal properties of cloud, their processes and precipitation pattern.

During pre-monsoon season, Arabian Sea gets influenced by dust storms mainly coming from middle-east and southwest Asia which may strongly vary concentration of aerosols (Babu et al. 2008; Prijith et al. 2013; Kaskaoutis et al. 2014). Various studies reported that highest mean seasonal aerosol loading gets influenced over Arabian Sea and Bay of Bengal during June–August, mainly due to dust storm (Satheesh et al. 2010). Major influence of dust particles especially mineral dust becomes important due to its interaction with water vapor in the atmosphere, which may alter hygroscopic nature of nuclei and hence their capability to form clouds (Tang et al. 2016). Mineral dust not only act as CCN but also as ice condensation nuclei, which also affects rate of ice nucleation in cloud. It has been explicitly studied in forming clouds as well as in climate models (Demott et al. 2010). During post-monsoon season, Arabian Sea is influenced by aerosols especially due to anthropogenic sources transporting from north-west part of Indian subcontinent (Tiwari et al. 2016). Researchers during Integrated Campaign for Aerosols, Gases and Radiation Budget (ICARB), showed that availability of aerosol is mainly associated with advection from western India and west Asia especially over Bay of Bengal (Badarinath et al. 2009). Moreover, Bay of Bengal consists fine mode aerosol mainly emitted from local land regions. Satellite retrievals also helped to show seasonal and inter-annual variation of aerosols over Arabian Sea and Bay of Bengal (Tiwari et al. 2016). Not only seasonal changes, but concentration of CCN, its nature as well as meteorological conditions play a significant role in varying cloud formation processes and hence cloud microphysical properties (Peng et al. 2002).

Various studies have been conducted over oceanic regions of India, which show long term SST with increasing trends may be due to global warming (Rao and Goswami 1987; Haroon and Afzal 2012; Pushpanjali et al. 2014). This warming signal may increase moisture content in the atmosphere, which may differ cloud microphysical properties and hence rainfall patterns over Indian subcontinent. Moreover, it is an agriculture dominant country and almost 60% of its population depends on agriculture for their livelihood

which contributes approximately 15.7% of India's Gross Domestic Product (GDP) (Aggarwal et al. 2010). About 700 million rural population of India directly and indirectly depends on climate sensitive sectors and also on natural resources for their livelihood (Sathaye et al. 2006). Monsoon is a seasonal reversing wind accompanied by south-west monsoon over most of the regions of India which provides ~ 70% of the annual mean precipitation (Kripalani et al. 2003; Turner and Annamalai 2012; Menon et al. 2013). This shows that high dependency of monsoon and its geographical location both plays a crucial role towards rainfall over India. Along with this, rising warming signals also contribute to vary various source conditions of cloud formation processes such as SST variabilities, changing rate of evaporation–condensation, concentration as well as type of cloud condensation nuclei and availability as well as amount of moisture content in the atmosphere. Such changes may alter cloud microphysical processes and hence rainfall patterns. Such changes in cloud processes can be well understood with the help of cloud microphysical property such as CER, which would determine the averaged size of cloud droplets (Zeng et al. 2014). The prime aim of this study is to see the impact of global warming on cloud properties, which in turn would affect cloud microphysical processes and hence cloud formation processes and rainfall patterns. So firstly, present study focuses to see long-term trend of SST over Indian Ocean to know the effect of global warming. Further study investigate the role of SST variabilities on moisture content with the help of SST-CER correlation. Like SST, alteration in AOD also influence the size distribution of cloud droplets. Thus, along with SST-CER correlation, study of AOD–CER correlation is also expected to show promising results to understand the impact of changes in SST as well as aerosol amount on size of cloud droplets.

2. Data and Methodology

2.1. Moderate Resolution Imaging Spectroradiometer (MODIS) Data

The Moderate Resolution Imaging Spectroradiometer (MODIS) is an imaging radiometer launched by The National Aeronautics and Space Administration (NASA) aboard the Terra (EOS AM) satellite in 1999 as well as aboard the Aqua (EOS PM) satellite in 2002. It can capture data in 36 spectral bands covering a wide spectral range from visible to thermal infrared bands (0.40–14.38 μm) which gives atmospheric, oceanic and terrestrial information (Savtchenko et al. 2004; Remer et al. 2005). Among them, visible and infrared bands help to determine cloud optical and microphysical properties (Saud et al. 2016). MODIS usually detects mid and high level clouds but usually finds difficult to capture low-level clouds. It has ability to detect optically thin clouds (< 14) and also can estimate clouds whose layer thickness is less than 1 km (Chan and Comiso 2011, Pincus and National Center for Atmospheric Research Staff 2019). For the selected study region, it is observed that almost all types of cloud are present over Indian Ocean but study would highly depend upon observation capabilities of MODIS (Dey et al. 2015). Specifically, mid and high-level cumulus and stratus type of clouds would be easily accessible by MODIS, whereas clouds undetected by MODIS will be missing in the present study. MODIS detect clear and cloudy conditions of each pixel depending on spatial variability (Ackerman et al. 1998). To get clear cloud pixel, two independent algorithms are applied to retrieve aerosol properties: deep blue method over land and dark target method over ocean. Ocean datasets are retrieved from the bands ranging from 0.47 to 2.13 μm (Remer et al. 2005). AOD of 0.55 μm using dark target method is usually used as it is a reliable wavelength reported for various climate studies as well as chemistry models (Kinne et al. 2003; Levy et al. 2007, 2010). Along with AOD, CER was also taken from MODIS which retrieve data at three near infrared bands (1.6 μm, 2.1 μm and 3.7 μm). CER of 3.7 μm band is comparatively better as it is minimally affected by cloud inhomogeneity and also absorbs solar radiation strongly (Rosenfeld et al. 2016). This band gives the information about the average size of water droplets from the top part of clouds, with a vertical penetration depth while other two bands—1.6 and 2.1 μm which contain more irradiance from lower cloud layers (Painemal and Zuidema 2011). Using bidirectional solar reflectance and near infrared absorption, CER gets retrieve with

the help of bi-spectral technique (Nakajima and King 1990). Cloud retrieval method of MODIS has advantage of differentiating liquid and ice phase to represent warm and cold cloud. On the other hand, it fails to collect only reflected irradiance of clouds and lacking in collecting vertical profile data (Tang et al. 2014). The error in MODIS retrieved CER is approximately less than 0.1 µm which has cloud optical thickness of 50 (King et al. 1997). Also, MODIS retrieved AOD has an expected error of $\pm (0.03 + 0.05AOD)$ over ocean (Remer et al. 2005). Present study uses level 3 monthly averaged data of AOD and CER from MODIS/Terra during 2001 to 2016, at spatial resolution of $1° \times 1°$ from Giovanni online portal which is developed and maintained by the National Aeronautics and Space Administration, Goddard Earth Sciences Data and Information Services Center (Acker and Leptoukh 2007; Giovanni 2019).

2.2. Centennial In Situ Observation Based Estimates (COBE) SST2 Data

The COBE data set is a spatially interpolated SST product available from 1850 to 2012 and was bias-adjusted up to 1941 using bucket correction (Ishii et al. 2005). Available COBE-SST2 measurements are buoy-based measurements which consists of pressure based sensors deployed beneath the water in fixed mounted locations. As pressure at the surface of water generates perturbation, the placed sensor measures it and attenuated with original pressure. The more attenuated the pressure, the smaller the wavelength of perturbation (Buoy 2019; Hirahara et al. 2014). This measurement of SST consists of ship and buoy observations only, which was gridded using optimal interpolation and prior to that was subjected for quality control. A typical SST measured by a ship has an uncertainty of about 1–1.5 K whereas a drifting buoy has a typical uncertainty of around 0.1–0.7 K (Reynolds et al. 2002). It conducts weather and climate research to observe as well as to understand earth's physical environment and also to improve weather and climate predictions on global to local scales.

Here long term (1960–2017) in situ data of SST is used to see the effect of global warming over Arabian Sea, Bay of Bengal and rest of the Indian Ocean. Monthly variation gridded long-term SST data is used

from web portal of the National Centers for Environmental Prediction (NCEP), Physical Science Division (PSD) at spatial resolution of $1° \times 1°$ (COBE-SST2 2017). Further monthly averaged seasonal data is used which also gets verified by various earlier studies (Ishii et al. 2005). Uncertainties in large scale average is considered to be small and has comparatively minor importance. SST data has large scale sampling uncertainty of about 0.01–0.02 °C during the year 1960–2000, which is usually small (Kennedy 2014).

2.3. Modern-Era Retrospective Analysis for Research and Applications (MERRA-2) Model Data

The MEERA-2 is a NASA atmospheric reanalysis data, made using an upgraded version of the Goddard Earth Observing System Model, Version 5 (GEOS-5). It is able to use newer microwave sounders, hyperspectral infrared radiance instruments as well as other data types. All data collections from MERRA-2 are provided on the same horizontal grid. This grid has 576 points in the longitudinal direction and 361 points in the latitudinal direction, corresponding to a resolution of $0.625° \times 0.5°$. It uses observation-based precipitation data as forcing for the land surface parameterization. This approach is similar to the gauge-based precipitation forcing developed for MERRA-Land (Reichle and Liu 2014). The forcing precipitation is not purely gauge observations, as it tapers back to MERRA-2 model generated precipitation. Monthly averaged data (2001–2016) of specific humidity at 850 hPa is used from Giovanni online data portal which is developed and maintained by the National Aeronautics and Space Administration, Goddard Earth Sciences Data and Information Services Center-NASA GES DISC (Acker and Leptoukh 2007; Giovanni 2019). Specific humidity is studied at 850 hPa to actually know the availability of moisture to CCN for cloud formation. Variation in moisture content at 850 hPa may affect droplet size distribution and hence cloud formation processes. Also, it has not been studied at other pressure levels as humidity is itself a highly varying parameter and analysis of it at all pressure levels is not required for the proposed study.

2.4. Study Area

The Intergovernmental Panel on Climate Change Fifth Assessment Report (IPCC AR5) reported that 90% of the heat due to global warming has been gathering in the oceans during last four decades (Rhein et al. 2014). It has been observed that this heat gets partially transferred which may cause the Indian Ocean as the warmest ocean among the major oceans and thus plays a critical role in regulating the climate and variability of the Asian monsoon as well as the dynamics over the tropical belt. Moreover, it is also reported that the warming trend over the Indian Ocean is a major player in influencing the overall trend of the global mean SST. During the past century, it is observed that the western Indian Ocean (5° S–10° N, 50° E–65° E) has warmed up tremendously which reaches up to the SST values of the warm pool. During 1901–2012, it is observed that the western Indian Ocean shows continuous warming since the start of twentieth century but attains an increasing rate after 1950s. For the rest of the Indian Ocean including warm pool region (20° S–20° N, 70° E–100° E), the warming gets pronounced only after 1950s (Roxy et al. 2014). Recent study reported that western Indian Ocean gets relatively cool while the rest of the Indian Ocean gets warmer including warm pool (with SST > 28 °C) during summer, which in turn would affect the annual mean SST (Roxy et al. 2015). The discovery of this dipole mode that accounts for about 12% of the sea surface temperature variability in the Indian Ocean—and in its active years, also causes severe rainfall in eastern Africa and droughts in Indonesia (Saji et al. 1999). Recent research study has reported that the Indo-Pacific warm pool (IPWP) 25° S–25° N and 40° E–130° W has warmed up substantially during the past century. The IPWP is considered to be the largest region of warm SSTs of the earth, highest rainfall and is fundamental to global atmospheric circulation and hydrological cycle. Changes in IPWP is due to natural as well as human contributions since 1950s simulated by climate model simulations using optimal fingerprint technique. Greenhouse gas forcing is found to be the dominant cause of the observed increases in IPWP intensity and size, whereas natural fluctuations associated with the Pacific Decadal

Oscillation have played a smaller yet significant role. Human-induced changes in the IPWP have important implications for understanding and projecting related changes in monsoonal rainfall, and frequency or intensity of tropical storms, which have profound socioeconomic consequences (Weller et al. 2016). This shows that Indian Ocean has lot of heterogeneity, which may alter source conditions for cloud formation processes. To understand this heterogeneity at high resolution, present study divides Indian Ocean into three parts as (a) Arabian Sea (AS) (9° N–19.07° N, 57.57° E–72.86° E), (b) Bay of Bengal (BOB) (6.33° N–15.82° N, 82° E–97.38 °E) and (c) Rest of Indian Ocean (IO) (5.80° N–60° S, 50.62° E–94.92° E) (Fig. 1). Long-term high spatial resolution studies will show the significant trends of SST over AS, BOB and IO can be expected with these divided regions.
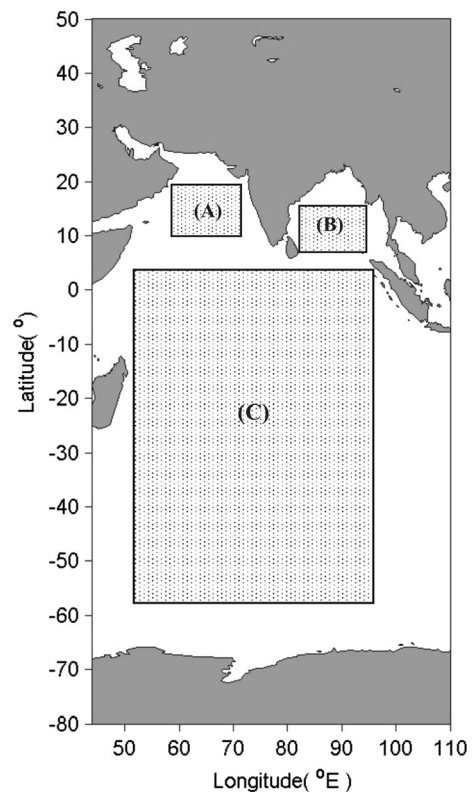

Figure 1
Study regions **a** AS, **b** BOB and **c** rest of IO for SST variation

3. Results and Discussion

Rise in SST due to advancement in global warming may alter source conditions of cloud formation, which in turn may affect cloud and rain formation processes. So to see the changes in cloud properties it is important to study variation in SST. Hence a long-term (1960–2017) annually averaged in situ SST data has been studied over oceanic regions of India, as mentioned in Figs. 1 and 2). Though SST show fluctuations over all the study areas but it shows an increasing trend with high confidence ($P < 0.05$). This P-value of < 0.05 shows more than 95% of level of confidence interval. It confirms the effect of global warming over the study regions, as the data of SST is comparatively large with 53 years. SST over AS (between 26.79 and 28.23 °C) and BOB (between 27.66 and 29.10 °C) shows an overall rise of about 0.11 °C/decade ($P < 0.05$), whereas IO (between 18.82 and 19.89 °C) shows an overall rise of about 0.14 °C/

decade ($P < 0.05$). All the SST trends have P-value less than 0.05, which shows that justifications used to interpolate values are more than 95% true. Along with P test, a non-parametric test named Mann–Kendall test is implemented to strengthen SST trends over AS, BOB and IO as it is commonly used to analyze long-term trends of meteorological variables (Kendall 1948; Gilbert 1987). This test do not assume any kind of distribution in the data as well as is insensitive for sudden missing data and thus can fit long-term trend systematically. Here, absence/presence of trend in the data is considered to be the null/alternate hypothesis. Same as P test, here Mann–Kendall test was also performed at 95% significance level. Using this test, Mann–Kendall statistic 'S' is obtained by calculating the difference between the number of positive and negative differences. In addition to it, Kendall's Tau coefficient 'τ' measures the strength and direction exist between two measured variables and it ranges from + 1 (indicates increasing trend) to -1 (indicates decreasing trend).
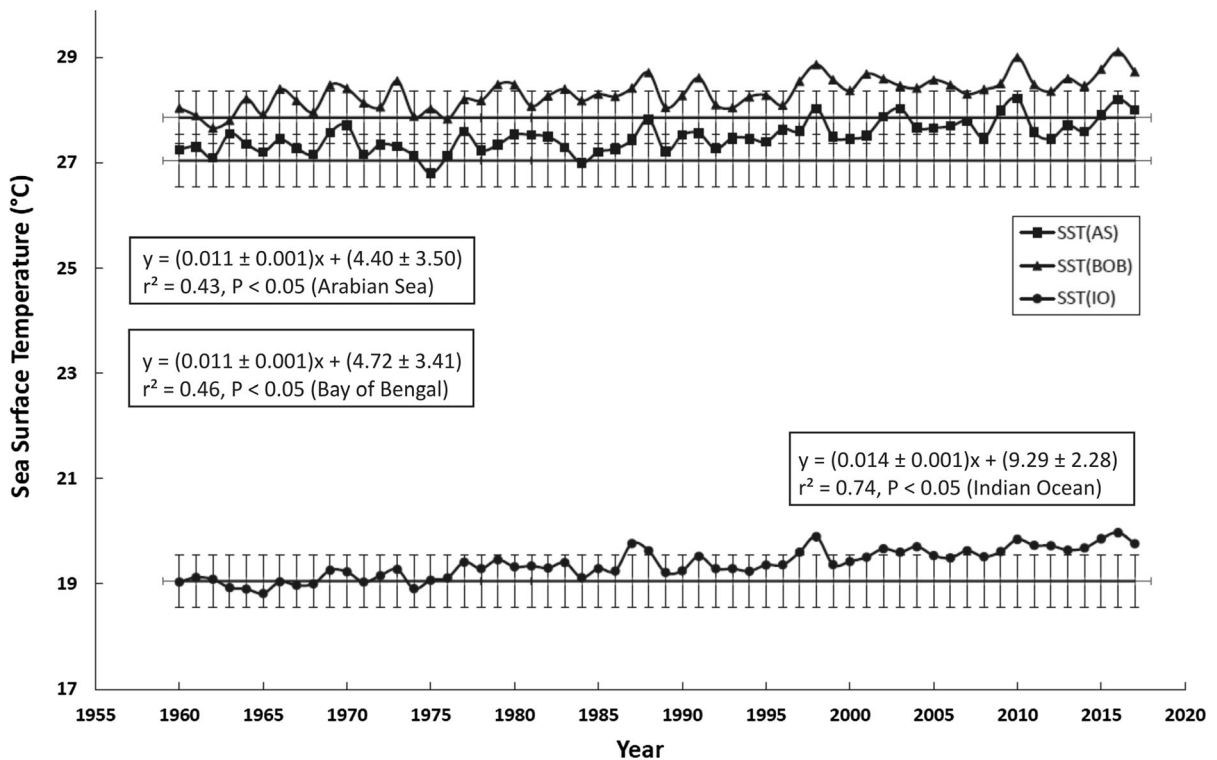

Figure 2
Long-term (1960–2017) annual temporal variation of *in-situ* SST over AS, BOB and rest of IO for the regions as defined in Fig. 1

Further, existence of the trend is governed with the help of standard test statistic 'Z'. Earlier research studies have reported that all these parameters of M–K test help to analyze long-term trends of climatic variables (Tabari et al. 2011; Gocic and Trajkovic 2013; Wang 2020; George and Athira 2020). For AS, S is 7.75×10^2 (i.e. positive) which depicts rise in SST with time. Same as S, values of τ (0.47) and Z (5.19) are also positive which altogether rejects null hypothesis and hence confirms an increasing trend at $P < 0.05$. Same as AS, BOB/IO also interprets similar kind of positive values for all these parameters, which are S ($7.95 \times 10^2/1.12 \times 10^3$), τ (0.48/0.67) and Z (5.33/7.49) and thus represents that SST rises with time from 1960–2017. Thus observed SST trends over the study region shows a high confidence and thus obtained results are highly reliable. High rate of increase of SST is observed over IO, may be due to presence of warm pool region in IO as compared to BOB and AS. Also the region selected for IO is bigger that includes some portions of northern tropical region, southern tropical regions and southern mid-latitude regions as compared to selected smaller regions of AS and BOB that include some portions of northern tropical region only.

Lower values of r^2 ($r^2_{AS} = 0.46$ and $r^2_{BOB} = 0.43$) signify more fluctuations in SST over AS and BOB whereas higher value of r^2 ($r^2_{IO} = 0.74$) is observed due to less SST variations in IO. This variation in r^2 values signifies that IO is warming faster than AS and BOB, as it has the effect of warm pool region and IO is also comparatively a bigger region which has less number of influencing parameters. On the other hand, selected AS and BOB may have more number of influencing parameters as they are located nearer to land surface. There are various factors such as presence of certain types of aerosol, difference in atmospheric pressure and temperature, warming effect of high surface temperature on ocean, interaction of atmosphere and ocean surface, variation in wind speed, temperature difference between surface and deep ocean waters, may affect SST more over AS and BOB as compared to IO. Though these oceanic regions are varying in nature as well as having different geographic locations but their long term annual trends show almost same rise of about 0.1 °C/decade with high confidence interval of > 95% and

$P < 0.05$, which is may be due to the warming climate.

Results have shown that long-term variation in SST is different over AS, BOB and IO, which shows that SST exhibit spatial and temporal changes. All the SST trends show an increasing trend and thus depict that SST rises year by year (Fig. 2). Along with temporal variation, spatial variation of SST can be studied with the help of linear interpolation at a grid of $1° \times 1°$ to understand the impact of global warming over oceanic regions of India (35° N–70° S, 45° E–95° E) (Fig. 3). Along with high resolution grid to grid interpretation, present study also show averaged seasonal variation [i.e. pre-monsoon (March, April and May), monsoon (June, July, August and September) and post-monsoon (October, November and December)] from 2001–2016 (IMD 2010).

Linear interpolation of SST helped to show seasonal variation which is clearly seen in Fig. 3. Higher temperature covers more area of tropical belt during pre-monsoon (Fig. 3a). On the other hand during monsoon, temperature declines with coverage of area (Fig. 3b) and for post-monsoon again patches of high temperature is visible over tropical regions (Fig. 3c). Tropical belt is capture with high temperature (20–30 °C) as compared to mid-latitude and polar regions (0–20 °C) (Fig. 3). High temperature over tropical regions may consist of more amount of moisture due to high rate of evaporation, whereas it decreases over mid-latitude regions followed by Polar Regions. As present study aims to perceive seasonal variability of SST on moisture content, linear interpolation of specific humidity at 850 hPa is studied at a spatial resolution of $1° \times 1°$ to know availability of moisture for CCN over oceanic regions of India (35° N–70° S, 45° E–95° E) (Fig. 4). Usually rise in SST is linked with vapor content in the atmosphere through high rate of evaporation. This may initiate cloud formation processes faster over ocean as it is the primary source of water vapor and almost 70% of the cloud forms over ocean (ISCCP NASA 2019; Earth observatory NASA 2020).

Along with seasonal distribution, tropical regions have more SST and specific humidity as compared to mid-latitude regions and polar regions which is clearly captured in Figs. 3 and 4. On the other hand,
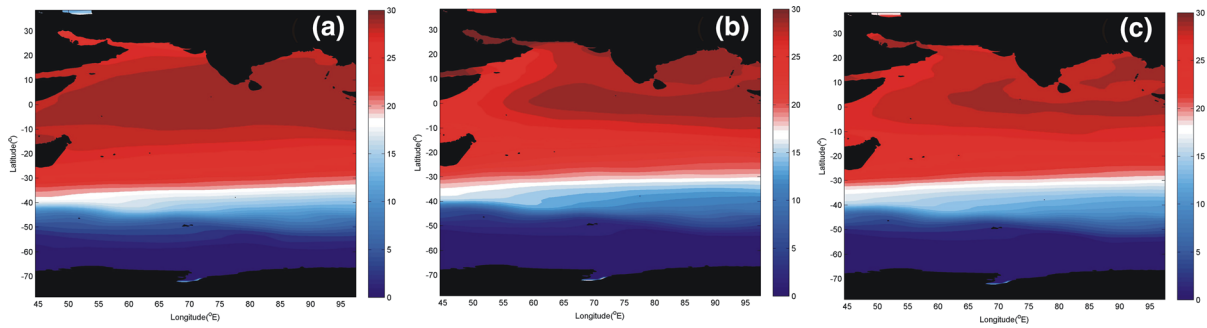
Figure 3
Color shading denotes grid wise linear interpolation of sea surface temperature (°C) at a spatial resolution of 1° × 1° during 2001–2016 for **a** pre-monsoon, **b** monsoon and **c** post-monsoon are shown over oceanic regions of India (35° N–70° S, 45° E–95° E)
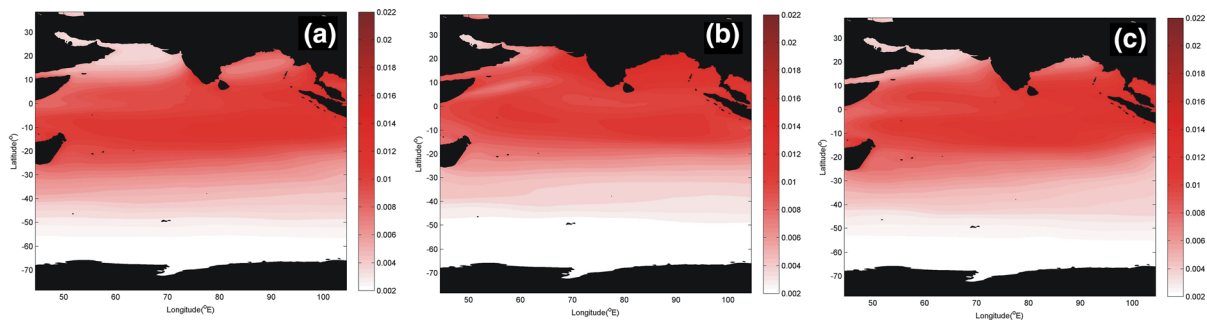

Figure 4
Color shading denotes grid wise linear interpolation of specific humidity (850 hPa) (kg/kg) at a spatial resolution of 1° × 1° during 2001–2016 for **a** pre-monsoon, **b** monsoon and **c** post-monsoon are shown over oceanic regions of India (35° N–70° S, 45° E–95° E)

low specific humidity and high SST is found over western Arabian Sea during pre-monsoon and post-monsoon that could be probably due to presence of low-pressure areas and strong winds (Raju et al. 2005). High specific humidity over tropics is due to high temperature, which in turn may increase rate of evaporation as well as condensation (Figs. 3, 4). Now more amount of liquid water droplets would get distributed among available CCN which may affect cloud microphysical properties. Present study captures monsoon activities with high specific humidity (∼ 0.01–0.018 kg/kg) over Arabian Sea, Bay of Bengal and southern tropical region which may increase size of cloud droplets through condensation, if concentration of CCN remains constant (Figs. 4b, c). As mentioned, present study focuses to see the effect of SST variabilities on size of cloud droplets by taking specific humidity and AOD into consideration. Study of such parameters may help to understand

cloud microphysical processes and their properties as well, under the effect of global warming. Hence, to interpret the role of SST on CER, seasonal correlation of SST-CER is studied at a spatial resolution of 1° × 1° with the help of linear grid wise interpolation over oceanic regions of India (Fig. 5). Seasonal SST-CER correlation plots show scattered pattern which means both these parameters have dependency of other parameters too, else it could be of uniform pattern. There are various factors affecting SST-CER correlation such as variation in SST, type of CCN, concentration of CCN, concentration of cloud droplets, change in CER, etc. Interpolation of correlated values consist of two types of patches-positive correlation and negative correlation. Positive correlation between SST and CER signifies that SST and size of cloud droplets are dependent on each other, whereas negative correlation depict that they have no mutual dependency (Wilks 2016). Further, lead-lag analysis
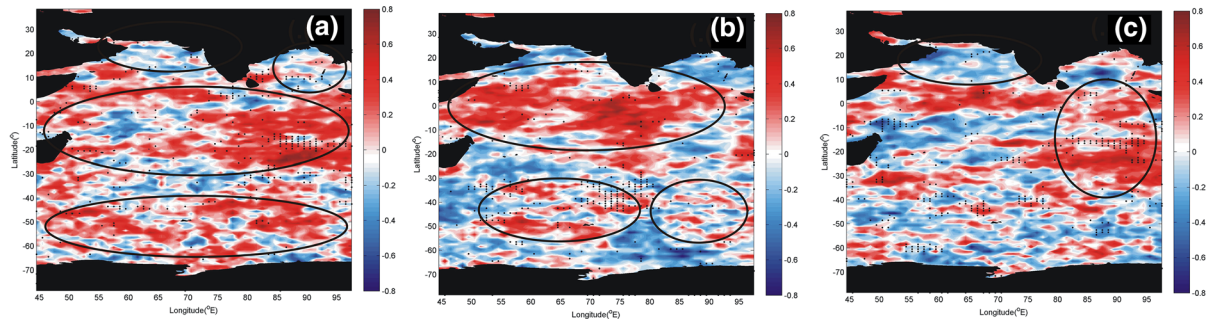
Figure 5
Color shading denotes grid wise linear correlation coefficients (r) between SST and CER during 2001–2016 for **a** pre-monsoon, **b** monsoon and **c** post-monsoon. Positive (~ 0.1 to ~ 0.8) and negative (~ -0.1 to ~ -0.8) correlation patches of SST-CER are shown over oceanic regions of India (35° N–70° S, 45° E–95° E). Black dots indicate the robustness of the interpolated correlation data derived from satellite with 95% significance level

is performed between correlation values of SST/AOD and CER which may depict strengthen positive and negative correlation. In Fig. 5, linear interpolation between SST and CER is shown and further to investigate the role of SST on CER, seasonal variation of aerosol concentration would be taken into consideration.

Studies have reported that concentration of aerosol is maximum during pre-monsoon, minimum during monsoon and moderate during post-monsoon over Bay of Bengal. On the other hand, Arabian Sea is highly influenced with south-west monsoon troughs and thus has higher concentration of aerosol compared to Bay of Bengal during all the seasons (Srivastava et al. 2012; Chen et al. 2017; Nizar and Dodamani 2019). Also, southern tropical and mid-latitude regions has less influence of aerosol and hence its impact can be neglected while SST-CER correlation study (MISR NASA 2019, Sikka 2018). During pre-monsoon, most of the Arabian Sea and Bay of Bengal show negative correlation from $\sim - 0.1$ to $\sim - 0.8$, which implies less moisture and higher CER (Figs. 4a, 5a). This could be possible when high concentration of aerosol (as in pre-monsoon) or specific types of hygroscopic nuclei are present. On the other hand, most of the southern tropical region get interpolated with positive ($\sim 0.1–0.8$) correlation which signifies the formation of bigger cloud droplets may be due to more moisture (Figs. 4a, 5a). Same as southern tropical region, southern mid-latitude region also gets interpolated

with positive correlation from ~ 0.1 to ~ 0.8, which depicts less moisture and smaller cloud droplets (Figs. 4a, 5a). These positive patches show linear dependency of moisture on CER, irrespective of aerosol loading, as these regions occupy low amount of aerosol and thus can be supposed to be a constant variable. Signature of south-west monsoon is captured with positive correlation ($\sim 0.1–0.8$) of SST-CER (Fig. 5b). This positive correlation depicts more moisture and bigger CER, considering least amount of aerosol concentration (Fig. 4b). Even the aerosol loading is less but concentration of CCN would be enough for moisture to form water cloud droplets with higher CER. As said earlier, availability of moisture over mid-latitude region might be enough to form small cloud droplets and thus captured with positive correlation ($\sim 0.1–0.8$) (Figs. 4b, 5b). During post-monsoon, negative correlation varies from $\sim - 0.1$ to $\sim - 0.8$ over Arabian Sea which implies less moisture and big cloud droplets, by assuming moderate amount of aerosol (Figs. 4c, 5c). On the other hand, effect of rising SST to increase CER is clearly captured with positive correlation ($\sim 0.1–0.8$) for retreating monsoon over Bay of Bengal as well as at higher longitudes of southern tropical regions (Fig. 5c). This dependency of SST on CER matches with high specific humidity depict the monsoonal effect (Fig. 4c. Also it helped to show the effect of warming signal on averaged size of cloud droplets, irrespective of their concentration. Hence, impact of high specific humidity is seen mostly by the

presence of bigger cloud droplets, which clearly states that moisture content has its impact on size of cloud droplets (positive correlation). On the contrary, less moisture tend to form big cloud droplets form and this could be possible due to presence of various types of CCN which further needs to be studied. However, interdependency between SST and CER is clearly visible over Indian Ocean but probably due to insufficient data, it is statistically weak at 95% significance level. Along with this, lead–lag analysis shows high value (0.02/0.02) for lead and low value (0.01/0.01) for lag during pre-monsoon/monsoon, which in turn depicts that positive correlation is more significant than negative correlation. On the other hand, the lead value is 0.01, which is smaller than lag value (0.02) and thus it shows that negative correlation is significant during post-monsoon.

SST or moisture content may has more prominent role towards size of cloud droplets as compared to AOD. Even if concentration of aerosol or CCN is low, amount of moisture play its major role on CER and that is important for the present study (Peng et al. 2002; Chylek et al. 2006). Any variation in CER would vary other cloud microphysical properties, cloud formation processes as well as rainfall. Thus to study the dependency of AOD on CER, linear grid wise interpolation is done seasonally over oceanic regions of India at a spatial resolution of $1° \times 1°$ and explained on the basis of lead–lag analysis (Fig. 6).

Positive correlation of AOD–CER implies more AOD and larger CER over most of the Indian Ocean may be due to high aerosol concentration during pre-monsoon season (Fig. 6a). Most of the Arabian Sea and Bay of Bengal show positive correlation ($\sim$ 0.1–0.8) of AOD–CER which implies high concentration of aerosols and big cloud droplets, that can be termed as a reverse secondary effect of aerosol or anti-twomey effect (Twomey 1974; Ma et al. 2018) (Fig. 6a). These positive correlation matches with negative correlation ($\sim - 0.1$ to $\sim - 0.8$) of SST-CER, which indicates bigger cloud droplets and less moisture may be due to presence of various types of CCN (Figs. 4a, 5a). Similarly, southern tropical region also interpolate with positive correlation ($\sim$ 0.1–0.8) of AOD–CER but with availability of more moisture as compared to Arabian Sea and Bay of Bengal (Figs. 4a, 6a). This excess amount of

moisture might be enough for various types of CCN to form bigger cloud droplets. South-west monsoonal features are captured with positive correlation ($\sim$ 0.1–0.8) of AOD–CER, which implies more aerosol and higher CER (Fig. 6b). Bigger cloud droplets in monsoon is may be due to more moisture, as captured with positive correlation ($\sim$ 0.1–0.8) of SST-CER (Figs. 4b, 5b). Thus, it shows a gradual shift in cloud droplet size distribution towards higher droplet diameters might be due to increasing specific humidity. In mid-latitude regions, availability of aerosol and specific humidity are less as compared to tropical regions which in turn tends to form small cloud droplets and thus captured with positive correlation ($\sim$ 0.1–0.8) of SST-CER and AOD–CER (Figs. 4b, 5b, 6b). During post-monsoon, most of the Arabian Sea interpolates with positive correlation ($\sim$ 0.1–0.8) of AOD–CER, which matches with negative correlation ($\sim - 0.1$ to $\sim - 0.8$) of SST-CER and thus depict big droplets due to more number of aerosol and less moisture may be due to presence of specific types of aerosol (Figs. 4c, 5c, 6c). During this season, onset of retreating monsoon has dependency of moisture on CER though have less number of aerosols as captured with negative correlation ($\sim - 0.1$ to $\sim - 0.8$) of AOD–CER and positive correlation ($\sim$ 0.1–0.8) of SST-CER over BOB (Figs. 4c, 5c, 6c). Thus correlation patches of AOD–CER clarifies the role of AOD on CER, which is also scattered and signifies dependency of other parameters along with SST and AOD. This is also observed with lead-lag analysis of AOD–CER for monsoon and pre-monsoon as the lead and lag values (0.01) are almost same, which shows that the correlation is nearly insignificant. For post-monsoon, the lead value (0.01) is smaller than lag value (0.02) which shows that negative correlation is more significant. Interdependency of such parameters at high resolution may help to know their impact on averaged size of cloud droplets. Such high spatial resolution study may help better to know the effect of global warming on various parameters such as activation of aerosols as well as availability of moisture content in the atmosphere which would help to understand cloud microphysical processes, their properties, precipitation pattern and hence regional climate variability. Further, this study needs to be verified with more
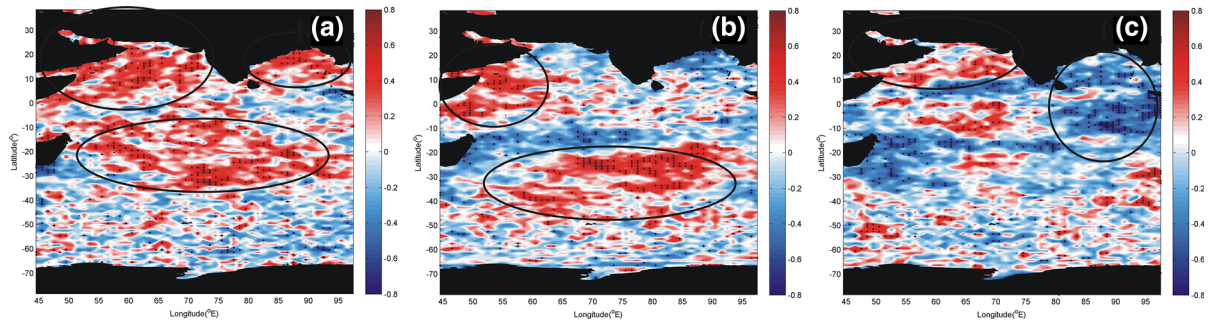
Figure 6

Color shading denotes grid wise linear correlation coefficients (r) between AOD and CER during 2001–2016 for **a** pre-monsoon, **b** monsoon and **c** post-monsoon. Positive ($\sim$ 0.1 to $\sim$ 0.8) and negative ($\sim$ − 0.1 to $\sim$ − 0.8) correlation patches of AOD–CER are shown over oceanic regions of India (35° N–70° S, 45° E–95° E). Black dots indicate the robustness of the interpolated correlation data derived from satellite with 95% significance level

number of parameters such as type of aerosol which would help to strengthen these correlation results under the effect of global warming.

4. Summary

Global warming is gradual increase in average temperature of the earth. Rise in SST is one of the effect of global warming which shows an increasing trend over selected regions of AS, BOB and rest of IO with the help of long -term (1960–2017) in situ annual averaged SST data. Though these oceanic regions have different geographic location but on an average have same rising rate (i.e. $\sim$ 0.1 °C/decade) using Mann–Kendall test, which is may be a reflecting effect of global warming. As most of the cloud forms over ocean, these warming signals may affect cloud microphysical processes and hence cloud microphysical properties such as CER. Present study focused to understand the source conditions of cloud microphysical processes at a spatial resolution of 1° × 1° along with seasonal variation over oceanic regions of India during 2001–2016 with the help of linear grid wise interpolation method. These interpolated patches have positive as well as negative correlation and is further analyzed with the help of lead-lag analysis. Rising SST may lead to increase moisture content and hence the size of cloud droplets, if aerosol concentration do not change with time. Signature of south-west monsoon as well as north-

east monsoon were captured with positive correlation ($\sim$ 0.1 to $\sim$ 0.8) of SST–CER, implies more moisture and higher CER again by assuming AOD as constant over AS and BOB respectively. Generally correlation does not change with spatial distribution but present grid to grid study region shows heterogeneity in SST-CER correlation during pre-monsoon, monsoon and post-monsoon. This dissimilarity in correlation is may be due to less number of parameters and less number of data points at each grid. To understand this non-uniformity in correlation patches, present study also focuses to see the role of AOD on CER, which also show heterogeneity and thus indicates that there might be role of other parameters too at regional scale affecting the size distribution of cloud droplets. During monsoon, less aerosol populated mid latitude region show positive correlation ($\sim$ 0.1 to $\sim$ 0.8) of AOD–CER and SST-CER which implies formation of small cloud droplets may be due to availability of moisture. Hence, SST-CER and AOD–CER correlation study signifies that both AOD and SST are efficient drivers to trigger cloud formation processes. This type of correlation study may play a significant role in understanding cloud microphysical properties, impact of global warming on cloud microphysical properties, their formation processes and hence precipitation patterns. Moreover studies on nature of aerosol are still sparse, more data on aerosol type may strengthen these results. Though these results are preliminary, more data and more parameters would help to build better statistics and

hence observed results could be more promising. Such study may help to understand regional climate variability and can be used as an input data in climate feedback models which further may help to improve simulation techniques and hence precipitation pattern.

Publisher's Note Springer Nature remains neutral with regard to jurisdictional claims in published maps and institutional affiliations.

REFERENCES

Acker, J. G., & Leptoukh, G. (2007). Online analysis enhances use of NASA earth science data. *Eos, Transactions American Geophysical Union, 88,* 14–17.

Ackerman, S. A., Strabala, K. I., Menzel, W. P., Frey, R. A., Moeller, C. C., & Gumley, L. E. (1998). Discriminating clear sky from clouds with MODIS. *Journal of Geophysical Research: Atmospheres, 103,* 32141–32157.

Aggarwal, P. K., Kumar, S. N., & Pathak. H. (2010). Impacts of climate change on growth and yield of rice and wheat in the Upper Ganga Basin. *WWF report*, pp 1–44.

Andreae, M. O. (1995). Climatic effects of changing atmospheric aerosol levels. *World Survey of Climatology, 16*(06), 347–398.

Andreae, M. O., Jones, C. D., & Cox, P. M. (2005). Strong present-day aerosol cooling implies a hot future. *Nature, 435,* 1187–1190.

Ansari, K., Pandithurai, G., & Kumar, V. A. (2020). Role of droplet size classes on the cloud droplet spectral dispersion as observed over the Western Ghats. *Atmospheric Research, 246,* 105104.

Aswini, A. R., Hegde, P., Aryasree, S., Girach, I. A., & Nair, P. R. (2020). Continental outflow of anthropogenic aerosols over Arabian Sea and Indian Ocean during wintertime: ICARB-2018 campaign. *Science of the Total Environment, 712,* 135214.

Babu, S. S., Nair, V. S., & Moorthy, K. K. (2008). Seasonal changes in aerosol characteristics over Arabian Sea and their consequence on aerosol short-wave radiative forcing: Results from ARMEX field campaign. *Journal of Atmospheric and Solar-Terrestrial Physics, 70,* 820–834.

Badarinath, K. V. S., Kharol, S. K., Sharma, A. R., & Prasad, V. K. (2009). Analysis of aerosol and carbon monoxide characteristics over Arabian Sea during crop residue burning period in the Indo-Gangetic Plains using multi-satellite remote sensing datasets. *Journal of Atmospheric and Solar-Terrestrial Physics, 71,* 1267–1276.

Bretherton, C. S., Blossey, P. N., & Jones, C. R. (2013). Mechanisms of marine low cloud sensitivity to idealized climate perturbations: A single-LES exploration extending the CGILS cases. *Journal of Advances in Modeling Earth Systems, 5*(2), 316–337.

Budhavant, K., Andersson, A., Holmstrand, H., Bikkina, P., Bikkina, S., Satheesh, S. K., & Gustafsson, Ö. (2020). Enhanced light-absorption of black carbon in rainwater compared with aerosols over the northern Indian Ocean. *Journal of Geophysical Research: Atmospheres, 125*(2), e2019JD031246.

Buoy (2019). Buoy-Based Wave Measurements by NexSens Technology available at https://www.nexsens.com/blog/buoy-based-wavemeasurements. Accessed 20 Sep 2019.

Chaboureau, J. P., Chédin, A., & Scott, N. A. (1998). Relationship between sea surface temperature, vertical dynamics, and the vertical distribution of atmospheric water vapor inferred from TOVS observations. *Journal of Geophysical Research: Atmospheres, 103*(D18), 23173–23180.

Chan, M. A., & Comiso, J. C. (2011). Cloud features detected by MODIS but not by CloudSat and CALIOP. *Geophysical research letters*, *38*(24), L24813.

Chen, J., Li, C., Ristovski, Z., Milic, A., Gu, Y., Islam, M. S., et al. (2017). A review of biomass burning: Emissions and impacts on air quality, health and climate in China. *Science of the Total Environment, 579,* 1000–1034.

Chylek, P., & Coauthors. (2006). Aerosol indirect effect over the Indian Ocean. *Geophysical Research Letters*, *33*, L06806.

COBE-SST2 (2017). Data provided by the NOAA/OAR/ESRL PSL, Boulder, Colorado, USA, from their Web site at https://psl.noaa.gov/. Accessed 05 Nov 2019.

DeMott, P. J., Prenni, A. J., Liu, X., Kreidenweis, S. M., Petters, M. D., Twohy, C. H., et al. (2010). Predicting global atmospheric ice nuclei distributions and their impacts on climate. *Proceedings of the National Academy of Sciences, 107*(25), 11217–11222.

Dey, S., Nishant, N., Sengupta, K., & Ghosh, S. (2015). Cloud climatology over the oceanic regions adjacent to the Indian Subcontinent: Inter-comparison between passive and active sensors. *International Journal of Remote Sensing, 36*(3), 899–916.

Earth observatory NASA (2020). *Earth observatory report by NASA* from their Web site at https://earthobservatory.nasa.gov/. Accessed 15 Sept 2020

Eck, T. F., Holben, B. N., Kim, J., Beyersdorf, A. J., Choi, M., Lee, S., et al. (2020). Influence of cloud, fog, and high relative humidity during pollution transport events in South Korea: Aerosol properties and PM2.5 variability. *Atmospheric Environment*, *232*, 117530.

Feingold, G., Koren, I., Wang, H., Xue, H., & Brewer, W. A. (2010). Precipitation-generated oscillations in open cellular cloud fields. *Nature, 466*(7308), 849–852.

Gabriel, R., Mayol-Bracero, O. L., & Andreae, M. O. (2002). Chemical characterization of submicron aerosol particles collected over the Indian Ocean. *Journal of Geophysical Research, 107,* 8005.

George, J., & Athira, P. (2020). Long-term changes in climatic variables over the Bharathapuzha river basin, Kerala, India. *Theoretical and Applied Climatology, 142,* 1–18.

Gilbert, R. O. (1987). *Statistical methods for environmental pollution monitoring*. New York: Wiley.

Giovanni (2019). *Data provided by the Earth Data, NASA, USA*. https://giovanni.gsfc.nasa.gov/. Accessed 30 Oct 2019.

Gocic, M., & Trajkovic, S. (2013). Analysis of changes in meteorological variables using Mann-Kendall and Sen's slope estimator statistical tests in Serbia. *Global and Planetary Change, 100,* 172–182.

Haroon, M. A., & Afzal, M. (2012). Spatial and temporal variability of sea surface temperature of the Arabian Sea over the past 142 years. *Pakistan Journal of Meteorology, 9*(17), 99–105.

Harrison, R. G., Nicoll, K. A., Ambaum, M. H., Marlton, G. J., Aplin, K. L., & Lockwood, M. (2020). Precipitation modification by ionization. *Physical Review Letters, 124*(19), 198701.

Hirahara, S., Ishii, M., & Fukuda, Y. (2014). Centennial-scale sea surface temperature analysis and its uncertainty. *Journal of Climate, 27,* 57–75.

IMD (2010). *Annual report by IMD,* Ministry of Earth Sciences, Govt. of India from their Web site at https://mausam.gov.in/ and https://imd.gov.in/.

IPCC. (2001). Climate Change 2001: The Scientific Basis. In J. T. Houghton, Y. Ding, D. J. Griggs, M. Noguer, P. J. van der Linden, X. Dai, et al. (Eds.), *Contribution of Working Group I to the Third Assessment Report of the Intergovernmental Panel on Climate Change* (p. 881). Cambridge: Cambridge University Press.

IPCC. (2007). Climate Change 2007: The Physical Science Basis. In S. Solomon, D. Qin, M. Manning, Z. Chen, M. Marquis, K. B. Averyt, et al. (Eds.), *Contribution of Working Group I to the Fourth Assessment Report of the Intergovernmental Panel on Climate Change*. Cambridge: Cambridge University Press.

IPCC, 2013: Summary for Policymakers. In: Climate Change 2013: The Physical Science Basis. In T. F. Stocker, D. Qin, G.-K. Plattner, M. Tignor, S. K. Allen, J. Boschung, A. Nauels, Y. Xia, V. Bex, & P. M. Midgley (Eds.), *Contribution of Working Group I to the Fifth Assessment Report of the Intergovernmental Panel on Climate Change*. United Kingdom and New York, NY, USA: Cambridge University Press, Cambridge.

ISCCP NASA (2019). *ISCCP report of NASA* from their Web site https://isccp.giss.nasa.gov/. Accessed 10 Dec 2019.

Ishii, M., Shouji, A., Sugimoto, S., & Matsumoto, T. (2005). Objective analyses of sea-surface temperature and marine meteorological variables for the 20th century using ICOADS and the KOBE collection. *International Journal of Climatology, 25,* 865–879.

Kaskaoutis, D. G., Kharol, S. K., Sinha, P. R., Singh, R. P., Kambezidis, H. D., Sharma, A. R., & Badarinath, K. V. S. (2011). Extremely large anthropogenic aerosol component over the Bay of Bengal during winter season. *Atmospheric Chemistry and Physics, 11,* 7851–7907.

Kaskaoutis, D. G., Rashki, A., Houssos, E. E., Goto, D., & Nastos, P. D. (2014). Extremely high aerosol loading over Arabian Sea during June 2008: The specific role of the atmospheric dynamics and Sistan dust storms. *Atmospheric Environment, 94,* 374–384.

Kendall, M. G. (1948). Rank correlation methods https://psycnet.apa.org/record/1948-15040-000. Accessed 13 Sep 2020

Kennedy, J. J. (2014). A review of uncertainty in in situ measurements and data sets of sea surface temperature. *Reviews of Geophysics, 52,* 1–32.

King, M. D., Tsay, S. C., Platnick, S. E., Wang, M., & Liou, K. N. (1997). Cloud Retrieval Algorithms for MODIS: Optical Thickness, Effective Particle Radius, and Thermodynamic Phase. *MODIS Algorithm Theoretical Basis Document No. ATBD-MOD-05 MOD06 – Cloud product, version 5*.

Kinne, S., et al. (2003). Monthly averages of aerosol properties: A global comparison among models, satellite data, and AERONET ground data. *Journal of Geophysical Research, 108,* 4634.

Kripalani, R. H., Kulkarni, A., Sabade, S. S., & Khandekar, M. L. (2003). Indian monsoon variability in a global warming scenario. *Natural Hazards, 29,* 189–206.

Levy, R. C., Remer, L. A., & Dubovik, O. (2007). Global aerosol optical properties and application to Moderate Resolution Imaging Spectroradiometer aerosol retrieval over land. *Journal of Geophysical Research, 112,* D13210.

Levy, R. C., Remer, L. A., Kleidman, R. G., Mattoo, S., Ichoku, C., Kahn, R., & Eck, T. F. (2010). Global evaluation of the Collection 5 MODIS dark-target aerosol products over land. *Atmospheric Chemistry and Physics, 10,* 10399–10420.

Lohmann, U., & Feichter, J. (2005). Global indirect aerosol effects: A review. *Atmospheric Chemistry and Physics, 5,* 715–737.

Ma, X., Jia, H., Yu, F., & Quaas, J. (2018). Opposite aerosol index-cloud droplet effective radius correlations over major industrial regions and their adjacent oceans. *Geophysical research letters, 45*(11), 5771–5778.

Menon, A., Levermann, A., Schewe, J., Lehmann, J., & Frieler, K. (2013). Consistent increase in Indian monsoon rainfall and its variability across CMIP-5 models. *Earth System Dynamics, 4,* 287–300.

MISR NASA (2019). Global and seasonal aerosol distributions from MISR from their Web site at https://earthobservatory.nasa.gov/. Accessed 02 Oct 2019.

Mitra, A. P., & Sharma, C. (2002). Indian aerosols: Present status. *Chemosphere, 49*(9), 1175–1190.

Muhsin, M., Sunilkumar, S. V., Ratnam, M. V., Parameswaran, K., Mohankumar, K., Mahadevan, S., et al. (2020). Contrasting features of tropospheric turbulence over the Indian peninsula. *Journal of Atmospheric and Solar-Terrestrial Physics, 197,* 105179.

Mukherjee, T., Vinoj, V., Midya, S. K., & Adhikary, B. (2020). Aerosol radiative impact on surface ozone during a heavy dust and biomass burning event over South Asia. *Atmospheric Environment, 223,* 117201.

Nageswararao, M. M., Sinha, P., Mohanty, U. C., & Mishra, S. (2020). Occurrence of More Heat Waves over the Central East Coast of India in the Recent Warming Era. *Pure and Applied Geophysics, 177*(2), 1143–1155.

Nakajima, T., & King, M. D. (1990). Determination of the optical thickness and effective radius of clouds from reflected solar radiation measurement Part I: Theory. *Journal of Atmospheric Science, 47,* 1878–1893.

Nizar, S., & Dodamani, B. M. (2019). Spatiotemporal distribution of aerosols over the Indian subcontinent and its dependence on prevailing meteorological conditions. *Air Quality, Atmosphere & Health, 12*(4), 503–517.

Painemal, D., & Zuidema, P. (2011). Assessment of MODIS cloud effective radius and optical thickness retrievals over the

Southeast Pacific with VOCALS-REx in situ measurements. *Journal of Geophysical Research, 116,* D24206.

Peng, Y., Lohmann, U., Leaitch, R., Banic, C., & Couture, M. (2002). The cloud albedo-cloud droplet effective radius relationship for clean and polluted clouds from RACE and FIRE.ACE. *Journal of Geophysical Research, 107,* 4106.

Pincus, R. & National Center for Atmospheric Research Staff (Eds.). (2019). *The Climate Data Guide: Cloud observations from MODIS. The climate data guide: Cloud observations from MODIS.* https://climatedataguide.ucar.edu/climate-data/cloud-observations-modis/. Accessed 20 Dec 2019.

Prijith, S. S., Rajeev, K., Thampi, B. V., Nair, S. K., & Mohan, M. (2013). Multi-year observations of the spatial and vertical distribution of aerosols and the genesis of abnormal variations in aerosol loading over the Arabian Sea during Asian summer monsoon season. *Journal of Atmospheric and Solar-Terrestrial Physics, 105–106,* 142–151.

Pushpanjali, B., Subrahmanyam, M., & Murty, K. V. (2014). Sea surface temperature and find later jet variations over Arabian Sea during summer monsoon. *Journal of Climatology and Weather Forecasting*, 2(2), 1000111.

Raju, P. V. S., Mohanty, U. C., & Bhatla, R. (2005). Onset characteristics of the southwest monsoon over India. *International Journal of Climatology: A Journal of the Royal Meteorological Society, 25*(2), 167–182.

Ramanathan, V., & Coauthors, . (2001). Indian Ocean Experiment: An integrated analysis of the climate forcing and effects of the great Indo-Asian haze. *Journal of Geophysical Research, 106,* 28371–28398.

Rao, K. G., & Goswami, B. N. (1987). Interannual variation of sea surface temperature over the Arabian Sea and the Indian monsoon: A new perspective. *American Meteorological Society, 116,* 558–568.

Reichle, R. H., & Liu, Q. (2014). *Technical Report Series on Global Modeling and Data Assimilation, Observation-Corrected Precipitation Estimates in GEOS-5, 35,* 1–18. (Available online at National Aeronautics and Space Administration, Goddard Space Flight Center Greenbelt, Maryland 20771)

Remer, L. A., et al. (2005). The MODIS aerosol algorithm, products, and validation. *Journal of Atmospheric Science, 62,* 947–973.

Reynolds, R., Rayner, N., Smith, T., Stokes, D., & Wang, W. (2002). An improved in-situ and satellite SST analysis for climate. *Journal of Climate, 15,* 1609–1625.

Rhein, M., et al. (2014). Observations: Ocean. In T. F. Stocker, et al. (Eds.), *Climate change 2013: The physical science basis* (pp. 255–315). Cambridge: Cambridge University Press.

Rosenfeld, D., et al. (2016). Satellite retrieval of cloud condensation nuclei concentrations by using clouds as CCN chambers. *Proceedings of the National Academy of Sciences, 113,* 5828–5834.

Roxy, M. K., Ritika, K., Terray, P., & Masson, S. (2014). The curious case of Indian Ocean warming. *Journal of Climate, 27,* 8501–8509.

Roxy, M. K., Ritika, K., Terray, P., & Masson, S. (2015). Indian Ocean warming–the bigger picture. *Bulletin of the American Meteorological Society, 96,* 1070–1072.

Saji, N. H., Goswami, B. N., Vinayachandran, P. N., & Yamagata, T. (1999). A dipole mode in the tropical Indian Ocean. *Nature*, *401*(6751), 360–363.

Sathaye, J., Shukla, P. R., & Ravindranath, N. H. (2006). Climate change, sustainable development and India: Global and national concerns. *Current Science, 90,* 314–325.

Satheesh, S. K., Vinoj, V., & Moorthy, K. K. (2010). Assessment of aerosol radiative impact over oceanic regions adjacent to Indian subcontinent using multisatellite analysis. *Advances in Meteorology, 2010,* 1–13.

Saud, T., Dey, S., Das, S., & Dutta, S. (2016). A satellite-based 13-year climatology of net cloud radiative forcing over the Indian monsoon region. *Atmospheric Research, 182,* 76–86.

Savtchenko, A., Ouzounov, D., Ahmad, S., Acker, J., Leptoukh, G., Koziana, J., & Nickless, D. (2004). Terra and Aqua MODIS products available from NASA GES DAAC. *Advances in Space Research, 34,* 710–714.

Schill, G. P., Froyd, K. D., Bian, H., Kupc, A., Williamson, C., Brock, C. A., et al. (2020). Widespread biomass burning smoke throughout the remote troposphere. *Nature Geoscience*, *13*, 422–427.

Shika, S., Gadhavi, H., Suman, M. N. S., Ravikrishna, R., & Gunthe, S. S. (2020). Atmospheric aerosol properties at a semi-rural location in southern India: Particle size distributions and implications for cloud droplet formation. *SN Applied Sciences, 2,* 1–15.

Sikka, D. R. (2018). Extreme weather and seasonal events during the Indian summer monsoon and prospects of improvement in their prediction skill under India's Monsoon Mission. *Dynamics and Predictability of Large-Scale, High-Impact Weather and Climate Events.* https://doi.org/10.1017/cbo9781107775541.026

Srivastava, A. K., Dey, S., & Tripathi, S. N. (2012). Aerosol characteristics over the Indo-Gangetic Basin: Implications to regional climate. *Atmospheric Aerosols-Regional Characteristics-Chemistry and Physics, 10,* 47782.

Stocker, T. F., Qin, D., Plattner, G. K., Tignor, M., Allen, S. K., & Boschung, J., et la. (2013). Climate change 2013: The physical science basis. *Contribution of working group I to the fifth assessment report of the intergovernmental panel on climate change,* p 1535.

Su, H., et al. (2017). Tightening of tropical ascent and high clouds key to precipitation change in a warmer climate. *Nature Communications, 8,* 1–9.

Tabari, H., Somee, B. S., & Zadeh, M. R. (2011). Testing for long-term trends in climatic variables in Iran. *Atmospheric Research, 100*(1), 132–140.

Tang, J., et al. (2014). Positive relationship between liquid cloud droplet effective radius and aerosol optical depth over Eastern China from satellite data. *Atmospheric Environment, 84,* 244–253.

Tang, M., Cziczo, D. J., & Grassian, V. H. (2016). Interactions of water with mineral dust aerosol: water adsorption, hygroscopicity, cloud condensation, and ice nucleation. *Chemical Reviews, 116*(7), 4205–4259.

Tarbuck, E. J., Lutgens, F. K., & Tasa, D. (1997). *The atmosphere: An introduction to meteorology, earth science.* New Jersey: Prentice Hall.

Tiwari, S., Mishra, A. K., & Singh, A. K. (2016). Aerosol Climatology over the Bay of Bengal and Arabian Sea Inferred from Space-Borne Radiometers and Lidar Observations. *Aerosol and Air Quality Research, 16,* 2855–2868.

Tiwari, S., Srivastava, A. K., Singh, A. K., & Singh, S. (2015). Identification of aerosol types over Indo-Gangetic Basin:

Implications to optical properties and associated radiative forcing. *Environment Science Pollution Research, 22,* 12246–12260.

Trenberth, K. E., & Shea, D. J. (2005). Relationships between precipitation and surface temperature. *Geophysical Research Letters*, *32*, L14703.

Turner, A., & Annamalai, H. (2012). Climate change and the South Asian summer monsoon. *Nature Climate Change, 2,* 587–595.

Twomey, S. (1977). The influence of pollution on the shortwave albedo of clouds. *Journal of Atmospheric Science, 34,* 1149–1152.

Vidya, P. J., Ravichandran, M., Subeesh, M. P., Chatterjee, S., & Nuncio, M. (2020). Global warming hiatus contributed weakening of the Mascarene High in the Southern Indian Ocean. *Scientific Reports, 10*(1), 1–9.

Wang, J. (2020). Determining the most accurate program for the Mann-Kendall method in detecting climate mutation. *Theoretical and Applied Climatology*, *142*, 847–854.

Weller, E., Min, S. K., Cai, W., Zwiers, F. W., Kim, Y. H., & Lee, D. (2016). Human-caused Indo-Pacific warm pool expansion. *Science advances, 2*(7), e1501719.

Wilks, D. (2016). "The stippling shows statistically significant grid points": How research results are routinely overstated and over interpreted, and what to do about it. *Bulletin of the American Meteorological Society, 97*(12), 2263–2273.

Zeng, S., Riedi, J., Trepte, C. R., Winker, D. M., & Hu, Y. X. (2014). Study of global cloud droplet number concentration with A-Train satellites. *Atmospheric Chemistry and Physics, 14,* 7125–7134.

Zheng, Y., Bourassa, M. A., & Ali, M. M. (2020). Statistical evidence on distinct impacts of short-and long-time fluctuations of Indian Ocean surface wind fields on Indian summer monsoon rainfall during 1991–2014. *Climate Dynamics, 54*(5), 3053–3076.